Alpha-Band Oscillations Enable Spatially and Temporally Resolved Tracking of Covert Spatial Attention

SCHOLARONE™
Manuscripts

Running Head: ALPHA OSCILLATIONS TRACK COVERT SPATIAL ATTENTION   1

Alpha-band oscillations enable spatially and temporally resolved tracking of covert spatial attention

Joshua J. Foster[1,2], David W. Sutterer[1,2], John T. Serences[3,4], Edward K. Vogel[1,2], & Edward Awh[1,2]

[1]Department of Psychology, The University of Chicago
[2]Institute for Mind and Biology, The University of Chicago
[3]Department of Psychology, University of California, San Diego
[4]Neuroscience Graduate Program, University of California, San Diego

Running Head: Alpha Oscillations Track Covert Spatial Attention

Key Words: spatial attention; EEG; alpha; oscillations; inverted encoding model

Conflict of Interest: None

Correspondence:
Joshua J. Foster or Edward Awh
Institute for Mind and Biology
University of Chicago
940 East 57th Street
Chicago, IL 60637
USA
Email: joshuafoster@uchicago.edu or awh@uchicago.edu

Abstract

Covert spatial attention is essential for our ability to direct limited processing resources to the relevant aspects of visual scenes. A growing body of evidence suggests that rhythmic neural activity in the alpha frequency band (8-12 Hz) tracks the spatial locus of covert attention, suggesting that alpha activity is integral to spatial attention. However, extant work has not provided a compelling test of another key prediction: that alpha activity tracks the *temporal dynamics* of covert spatial orienting. Here, we examined the time-course of spatially specific alpha activity following central cues and during visual search. Critically, the time-course of this activity tracked trial-by-trial variations in orienting latency during visual search. These findings provide important new evidence for the link between rhythmic brain activity and covert spatial attention, and highlight a powerful approach for tracking the spatial and temporal dynamics of this core cognitive process.

ALPHA OSCILLATIONS TRACK COVERT SPATIAL ATTENTION   3

A typical visual scene contains more information than an observer can process at once. Therefore, we must focus limited processing resources on the most relevant aspects of the environment. Spatial attention plays a central role in this effort, enhancing the quality and speed of processing at attended locations (Carrasco & McElree, 2000; Eriksen & Hoffman, 1974; Posner, 1980; for review, see Carrasco, 2011). Because spatial attention is essential for normal perceptual function, there is great interest in understanding the neural basis of this process. One promising approach has been to examine the links between attentional states and rhythmic brain activity. A growing body of evidence suggests that oscillatory activity in the alpha frequency band (8-12 Hz) is integral to covert spatial attention. Measurements of the topographic distribution of alpha power on the scalp have revealed that alpha power is reduced contralateral to an attended location (e.g., Kelly, Lalor, Reilly, & Foxe, 2006; Sauseng et al., 2005; Thut, Nietzel, Brandt, & Pascual-Leone, 2006). Further work has shown that the topography of alpha power tracks not just the hemifield but also the specific location that an observer is attending (e.g., Bahramisharif, van Gerven, Heskes, & Jensen, 2010; Rihs, Michel, & Thut, 2007; Worden, Foxe, Wang, & Simpson, 2000). These findings suggest that spatially specific alpha-band activity directly tracks the deployment of spatial attention (Foxe & Snyder, 2011; Jensen & Mazaheri, 2010).

Nevertheless, the hypothesis that alpha activity is integral to spatial attention makes a clear prediction that remains untested: The topography of alpha-band activity should track not only the spatial locus of attention but also the time-course of covert orienting. Extant studies have not provided a rigorous analysis of the time-course of spatially specific alpha activity, or examined whether this time-course of this activity tracks variations in the latency of covert

ALPHA OSCILLATIONS TRACK COVERT SPATIAL ATTENTION   4

spatial orienting. Thus, our goal was to determine whether dynamic changes in alpha-band

activity provide a sensitive index of the speed of covert spatial orienting.

Figure 1. Inverted encoding method for reconstructing spatial channel tuning functions (CTFs) from the pattern of alpha-band (8-12 Hz) power across the scalp. We modeled alpha power measured at each electrode as the weighted sum of eight spatially tuned channels (a). Each curve shows the predicted response of one of the channels across eight possible attended angular locations. In a training phase (b), we estimated a set of channel weights that characterize the relative contributions of each of the spatial channels to the response measured at each of the scalp electrodes. In a test phase (c), using an independent set of data, we used the channel weights to estimate the channel responses from the observed pattern of alpha power on the scalp. The resulting channel tuning function (CTF) reflects the spatial selectivity of population-level alpha power, as measured with EEG.

ALPHA OSCILLATIONS TRACK COVERT SPATIAL ATTENTION   5

To this end, we used EEG recordings and an inverted encoding model (IEM; Brouwer &

Heeger, 2009; Sprague & Serences, 2013; for review, see Sprague, Saproo, & Serences, 2015) to

examine the time-course of spatially specific alpha-band activity. This approach assumes that the

topographic pattern of alpha power across the scalp reflects the activity of a number of

underlying spatially tuned channels (or neuronal populations; Fig. 1a). By first estimating the

relative contributions of these channels to each electrode on the scalp (Fig. 1b), the model can

then be *inverted* so that the underlying response of these spatial channels can be estimated from

the pattern of alpha power across the scalp (Fig 1c). The resulting profile of responses across the

spatial channels (termed channel tuning functions or CTFs) reflect the spatial tuning of

population-level alpha power, as measured with EEG. Thus, the IEM approach enables a

straightforward quantification of spatially selective activity from a higher-dimensional pattern of

alpha power on the scalp. By performing this analysis across separate points in time, we were

able to examine the temporal dynamics of spatially selective alpha-band activity (also see,

Foster, Sutterer, Serences, Vogel, & Awh, 2016; Samaha, Sprague & Postle, 2016).

In Experiment 1, we showed that alpha CTFs tracked the attended location following an

attention-directing cue during a spatial cueing task. Dovetailing with behavioral estimates of the

latency of endogenous orienting (e.g., Müller & Rabbit, 1998), we found that the topographic

distribution of alpha power tracked the cued location starting approximately 300 ms after the

central, attention-directing cue, revealing the shift of covert attention to the cued location. In

Experiment 2, we manipulated the latency of covert orienting by varying the difficulty of a visual

search task. Spatially specific alpha activity that tracked the target location had a faster rise time

in trials in which target selection was fastest, providing clear evidence that alpha-band activity

reveals the temporal dynamics of spatial attention. These results provide a critical extension to

the evidence linking alpha band activity with spatial attention by demonstrating that dynamic

changes in the topography of alpha activity track the latency of covert spatial orienting.

Moreover, this approach provides a powerful new tool for achieving spatially and temporally-

resolved measurements of this core cognitive process.

General Method

Subjects

Fifty volunteers (20 in Experiment 1, and 30 in Experiment 2[1]) participated in the

experiments for monetary compensation ($10/hr). Subjects were between 18 and 35 years old,

reported normal or corrected-to-normal visual acuity, and provided informed consent according

to procedures approved by the University of Oregon Institutional Review Board.

In Experiment 1, subjects were excluded from all analyses if fewer than 700 trials

remained after discarding trials contaminated by recording or ocular artifacts. This exclusion

criterion was set during data collection, and was chosen based on our work using the IEM

method to track locations stored in WM (Foster et al., 2016). Two subjects were excluded due to

excessive artifacts, and two subjects were excluded due to an error with stimulus presentation

leaving a total of 16 subjects.[2] All subjects in the final sample had at least 700 artifact-free trials

($M = 1165$, $SD = 173$).

In Experiment 2, subjects were excluded from analyses if fewer than 600 trials per

condition (easy search or hard search) remained after discarding trials with artifacts and/or

incorrect responses. We relaxed the exclusion criterion in Experiment 2 because we obtained

fewer trials per condition because Experiment 2 included two conditions rather than one. The

exclusion criterion was determined during the course of data collection but before the data were

analyzed. Seven subjects were excluded due to excessive artifacts, leaving a total of 23 subjects.[3]

ALPHA OSCILLATIONS TRACK COVERT SPATIAL ATTENTION   7

All subjects in the final sample had at least 600 trials per search condition ($M = 772$, $SD = 79$)

after artifacts and incorrect responses were discarded.

Apparatus and Stimuli

We tested subjects in a dimly lit, electrically shielded chamber. Stimuli were generated

using Matlab (Mathworks) and the Psychophysics Toolbox (Brainard, 1997; Pelli, 1997) and

were presented on a 17-in CRT monitor (refresh rate: 60 Hz) at a viewing distance of ~100 cm.

Stimuli were rendered in dark grey against a medium gray background.

Procedures

After providing informed consent, subjects were fitted with a cap embedded with 20

scalp electrodes before completing the experimental task. Experiment 1 took approximately 3

hours to complete, and Experiment 2 took approximately 3.5 hours to complete (including

preparation time and experimental time).

Experiment 1: Spatial cueing task. Subjects in Experiment 1 completed a spatial cueing

task in which they were required to identify a target digit among distractor letters (Fig. 2a).

Subjects initiated each trial with a spacebar press. Each trial began with a central fixation point

(0.24° in diameter), surrounded by equally spaced placeholder rings (1.7° in diameter, rim was

0.08° thick). Each placeholder was centered 2.4° from the fixation point. The exact angular

position of the placeholders were jittered on each trial within a 45° wedge. Thus, the position of

the first placeholder varied between -22.5° and 22.5°, the second varied between 22.5° and 67.5°,

and so on. This jitter was not necessary for the IEM analysis, and stimulus positions were not

jittered in Experiment 2 (details below). After a variable interval between 800 and 1500 ms, a

central cue (87.5% valid), presented for 250 ms, indicated the likely location of a subsequent

target. The cue was a small cross (0.6° wide, arms were 0.08° thick) with three green arms and

ALPHA OSCILLATIONS TRACK COVERT SPATIAL ATTENTION   8

one blue arm (or vice versa, counterbalanced across observers). The uniquely colored arm of the

cue pointed towards the cued placeholder. A target display was presented 1250 ms after cue

onset in which each placeholder was occupied by a letter or digit. The display included one

target (a digit between 1 and 9) among distractors (uppercase letters). Digits and letters were

approximately 0.9° tall and 0.8° wide. The distractor letters were randomly selected without

replacement from all possible letters (except for I, S, and Z because of their similarity to the

digits 1, 5, and 2, respectively). The target was backwards masked with a # symbol presented for

400 ms. Following the mask, subjects made an unspeeded report of the target identity using the

numberpad on a standard keyboard. The reported digit appeared ~1° above the fixation point,

and subjects could correct their response if they pressed a wrong key. Finally, subjects confirmed

their response with a spacebar press.

     To encourage subjects to attend the cued location in advance of the target display, and we

adjusted the duration of the target display for each subject using a staircase procedure. Subjects

completed 1-2 blocks (72 trials per block) blocks of this procedure at the start of the session.

During the staircase procedure, the cue was valid on all trials during the staircase procedure, and

subjects were instructed to attend the cued location. Exposure duration was decreased by 16.7 ms

(i.e., one refresh cycle at 60 Hz) when subjects made a correct response or increased by 33.3 ms

(i.e., two refresh cycles at 60 Hz) when subjects made an incorrect response, until performance

reached an asymptote. The resulting duration of the target display varied between 33.3 ms and

66.7 ms across subjects. This staircase procedure was somewhat coarse because changing

exposure duration by 16.7 ms had a considerable effect on task difficulty. Nevertheless, this

procedure ensured that the target identification was adequately difficult for all subjects: target

identification accuracy ranged between 65.7% and 97.0% (M = 83.5%, SD = 9.5%) on validly

ALPHA OSCILLATIONS TRACK COVERT SPATIAL ATTENTION   9

cued trials, and all subjects showed a large spatial cueing effect, ranging between 26.6% and

69.8% ($M = 46.6\%$, $SD = 13.0\%$).

Following the staircase procedure, subjects completed 20 blocks of 72 trials, or as many

blocks as time permitted (all subjects completed at least 13 blocks), of the spatial cueing task.

Each of the eight placeholders were cued equally often within each block of trials.

Experiment 2: Visual search task. Subjects in Experiment 2 performed a visual search

task in which they searched for a target (a vertical or horizontal bar) among distractors (Fig. 3a).

Each item in the search display consisted of a dark grey bar ($1.5° \times 0.2°$) superimposed on a grey

circle (2.1° in diameter). The items were equally spaced in a circle around a dark grey fixation

point (0.2° in diameter). Each item was centered 3° from the fixation point.

We varied the difficulty of visual search by manipulating both *distractor variability* (i.e.,

uniform vs. varied distractor orientations) and *target-distractor similarity* (i.e., the extent to

which the distractors resemble the target). In the easy search condition, all distractors were

identical and were rotated 45° clockwise or counter clockwise from the possible target

orientations (vertical and horizontal; Fig. 3a). Thus, distractor variability and target-distractor

similarity were low. In the hard search condition, the distractors were heterogeneous, and were

rotated 22.5° from the possible target orientations (Fig. 3a). Thus, distractor variability and

target-distractor similarity were higher than in the easy search condition, resulting in a more

difficult search (Duncan & Humphreys, 1989).

Each search array was presented for 2 seconds, separated by a variable intertrial interval

between 1.8 and 2.3 seconds, during which only the fixation point remained visible. Observers

reported whether the target was vertical or horizontal by pressing the "z" key (left index finger)

or "/?" key (right index finger), respectively. Subjects were instructed to respond as quickly and

ALPHA OSCILLATIONS TRACK COVERT SPATIAL ATTENTION   10

accurately as possibly, and feedback (mean RT and accuracy) was provided at the end of each

block of trials. To minimize artifacts during the stimulus display and a 300 ms pre-stimulus

baseline period, subjects were instructed to maintain fixation throughout each block of the search

task, and to blink (if necessary) immediately after the offset of the search array.

Subjects completed 30 blocks of 64 trials. The search conditions (easy vs. hard) were

blocked, and the conditions alternated between blocks. The order of the conditions (easy-hard-

easy-hard or hard-easy-hard-easy) was counterbalanced across subjects. Before beginning the

session, subjects completed two blocks of practice trials (easy search followed by hard search).

Each subject also completed a short practice session the day before testing to familiarize them

with the visual search task the day before the EEG session. During this session, subjects

completed three blocks of the easy search condition followed by three blocks of the hard search

condition.

Electrophysiology

EEG was recorded using 20 tin electrodes mounted in an elastic cap (Electro-Cap

International, Eaton, OH). We recorded from International 10/20 sites F3, FZ, F4, T3, C3, CZ,

C4, T4, P3, PZ, P4, T5, T6, O1, and O2, along with five nonstandard sites: OL midway between

T5 and O1, OR midway between T6 and O2, PO3 midway between P3 and OL, PO4 midway

between P4 and OR, and POz midway between PO3 and PO4. All sites were recorded with a

left-mastoid reference, and were re-referenced offline to the algebraic average of the left and

right mastoids. To detect horizontal eye movements, horizontal electrooculogram (EOG) was

recorded from electrodes placed ~1 cm from the external canthus of each eye. To detect blinks

and vertical eye movements, vertical EOG was recorded from an electrode placed below the

right eye and referenced to the left mastoid. The EEG and EOG were amplified with an SA

ALPHA OSCILLATIONS TRACK COVERT SPATIAL ATTENTION   11

Instrumentation amplifier with a bandpass of 0.01 to 80 Hz and were digitized at 250 Hz using

LabVIEW 6.1 running on a PC. Trials were visually inspected for artifacts, and we discarded

trials (both EEG and behavioral data) contaminated by blocking, blinks, detectable eye

movements, excessive muscle noise, or skin potentials. Removal of ocular artifacts was

effective: variation in the grand-averaged HEOG waveforms by cued/target locations was < 3

µV. Given that eye movements of about 1° of visual angle produce a deflection in the HEOG of

approximately 16 µV (Lins, Picton, Berg, & Scherg, 1993), the residual variation in the average

HEOG corresponds to variations in eye position of <0.2° of visual angle (i.e., smaller than the

size of the fixation point).

Time-Frequency Analysis

Time-frequency analyses were performed using Matlab's Signal Processing toolbox

(Mathworks) and EEGLAB toolbox (Delorme & Makeig, 2004). To isolate frequency-specific

activity, the raw EEG signal was bandpass filtered using a two-way least-squares finite impulse

response filter ('eegfilt.m' from EEGLAB Toolbox; Delorme & Makeig, 2004). This filtering

method uses a zero-phase forward and reverse operation, which ensures that phase values are not

distorted, as can occur with forward-only filtering methods. A Hilbert Transform (Matlab Signal

Processing Toolbox) was applied to the bandpass-filtered data, producing the complex analytic

signal, $z(t)$, of the filtered EEG, $f(t)$ where $z(t) = f(t) + i\tilde{f}(t) = A(t)e^{i\varphi(t)}$, from which

instantaneous amplitude, $A(t)$, was extracted; $\tilde{f}(t)$ is the Hilbert Transform of $f(t)$ and $i =$

$\sqrt{-1}$. The complex analytic signal was extracted for each electrode using the following Matlab

syntax:

```
hilbert(eegfilt(data,F,f1,f2)')'
```

where data is a 2D matrix of raw EEG (number of trials × number of samples), F is the sampling

frequency (250 Hz), f1 is the lower bound of the filtered frequency band, and f2 is the upper

bound of the filtered frequency band. For alpha-band analyses, we used an 8-12 Hz bandpass

filter, thus f1 and f2 were eight and twelve, respectively. For the time-frequency analysis, we

searched a broad range of frequencies (4-50 Hz, in increments of 1 Hz with a 1 Hz bandpass).

For these analyses f1 and f2 were four and five to isolate 4-5 Hz activity, five and six to isolate

5-6 Hz activity, and so on. Power was computed by squaring the complex magnitude of the

complex analytic signal, which was then averaged across trials.

Artifact-free trials were partitioned into three blocks for the inverted encoding model

(two training blocks, one testing block; see Inverted Encoding Model for details). To prevent

bias in our analysis, we equated the number of observations across locations within each block,

and between conditions in Experiment 2. To this end, we calculated the minimum number of

trials for any given cued/target location, *n*, for each participant, and assigned *n*/3 many trials for

each location to each of the three blocks. Importantly, the blocks were independent (i.e., no trial

was repeated across blocks) to prevent circularity in the cross-validation procedures used for the

IEM routine (see Inverted Encoding Model). Power was then calculated for each location for

each block, resulting in an $l*b \times m \times s$ matrix of power values, where l is the number of

locations, b is the number of blocks, m is the number of electrodes, and s is the number of time

samples. For the analysis in which the IEM is applied across many frequency bands, we down-

sampled the data matrix of power values to a sample rate of 50 Hz (i.e., one sample every 20 ms)

to reduce computation time. We down-sampled the matrix of power values (i.e., after filtering

and applying the Hilbert transform) so that down-sampling did not affect how power values were

obtained. The data matrix was not down-sampled for analyses restricted to the alpha band.

ALPHA OSCILLATIONS TRACK COVERT SPATIAL ATTENTION   13

Finally, because we equated the number of trials across locations within blocks, a random

subset of trials were not included in any block. We randomly generated multiple block

assignments (five for the full time-frequency analyses, ten for the alpha-band analyses, and 100

for the latency analyses in Experiment 2), each resulting in an $l*b \times m \times s$ power matrix. The

IEM routine (see Inverted Encoding Model) was applied to the matrices of power values for each

block assignment, and their outputs (i.e., channel response profiles) were averaged. This iterative

approach better utilized the complete data set for each participant and reduces noise in the

resulting CTFs by minimizing the influence of idiosyncrasies in estimates of power specific to

any given assignment of trials to blocks.

Inverted Encoding Model

Following our previous work on spatial working memory (Foster et al., 2016), we used

an IEM to reconstruct location-selective CTFs from the topographic distribution of oscillatory

power across electrodes. We assumed that power measured at each electrode reflects the

weighted sum of eight spatial channels (i.e., neuronal populations), each tuned for a different

angular location (c.f. Brouwer & Heeger, 2009; Sprague & Serences, 2013). We modeled the

response profile of each spatial channel across angular locations as a half sinusoid raised to the

seventh power, given by:

$$R = \sin(0.5\theta)^7$$

where θ is angular location (ranging from 0° to 359°), and R is the response of the spatial

channel in arbitrary units. This response profile was circularly shifted for each channel such that

the peak response of each spatial channel was centered over one of the eight locations

(corresponding to the cued/target locations: 0°, 45°, 90° etc. for Experiment 1; and 22.5°, 67.5°,

112.5° etc. for Experiment 2; see Fig. 1a).

ALPHA OSCILLATIONS TRACK COVERT SPATIAL ATTENTION   14

An IEM routine was applied to each time-frequency point in the time-frequency analyses, and to each time point in the alpha-band analyses. This routine proceeded in two stages (train and test). In the training stage (Fig. 1b), training data B_1 were used to estimate weights that approximate the relative contribution of the eight spatial channels to the observed response measured at each electrode. Let B_1 (m electrodes $\times$ n_1 observations) be the power at each electrode for each measurement in the training set, C_1 (k channels $\times$ n_1 observations) be the predicted response of each spatial channel (determined by the basis functions) for each measurement, and W (m electrodes $\times$ k channels) be a weight matrix that characterizes a linear mapping from "channel space" to "electrode space". The relationship between B_1, C_1, and W can be described by a general linear model of the form:

$$\mathbf{B_1 = WC_1}$$

The weight matrix was obtained via least-squares estimation as follows:

$$\widehat{\mathbf{W}} = \mathbf{B_1 C_1}^{\mathbf{T}}\left(\mathbf{C_1 C_1}^{\mathbf{T}}\right)^{-1}$$

In the test stage (Fig. 1c), with the weights in hand, we inverted the model to transform the observed test data B_2 (m electrodes $\times$ n_2 observations) into estimated channel responses, C_2 (k channels x n_2 observations):

$$\widehat{\mathbf{C_2}} = \left(\widehat{\mathbf{W}}^{\mathbf{T}}\widehat{\mathbf{W}}\right)^{-1}\widehat{\mathbf{W}}^{\mathbf{T}}\mathbf{B_2}$$

Each estimated channel response function was circularly shifted to a common center (i.e., 0° on the "Channel Offset" axes of the figures) by aligning the estimated channel responses to the channel tuned for the cued/target location to yield CTFs. The IEM routine was performed separately for each time point.

Importantly, we used a "leave-one-out" cross validation routine such that two blocks of estimated power values (see Time-Frequency Analysis) served as B_1 and were used to estimate

ALPHA OSCILLATIONS TRACK COVERT SPATIAL ATTENTION   15

$\hat{W}$, and the remaining block served as B_2 and was used to estimate C_2, ensuring that the training

and test data were always independent. This process was repeated until each of the three blocks

were held out as the test set, and the resulting CTFs were averaged across each test block.

Finally, because the exact contributions of each spatial channel to each electrode (i.e., the

channel weights, W) will likely vary by subject, the IEM routine is applied separately for each

subject, and statistical analyses were performed on the reconstructed CTFs. This approach

allowed us to disregard differences in the how location-selective activity is mapped to scalp-

distributed patterns of power across subjects, and instead focus on the profile of activity in the

common stimulus or "information" space (Foster et al., 2016; Sprague et al., 2015).

Statistical Analysis

Quantifying CTF selectivity. To quantify the location selectivity of CTFs, we used linear

regression to estimate CTF slope (i.e., slope of channel response as a function of location

channels after collapsing across channels that were equidistant from the channel tuned to the

location of the evoking stimulus). Higher CTF slope indicates greater location selectivity.

Permutation testing. In Experiment 1, to test whether CTF selectivity was reliably above

chance, we tested whether CTF slope was greater than zero using a one-sample t test. Because

mean CTF slope may not be normally distributed under the null hypothesis, we employed a

Monte Carlo randomization procedure to empirically approximate the null distribution of the t

statistic. Specifically, we implemented the IEM as described above but randomized the location

labels within each block so that the labels were random with respect to the observed responses in

each electrode. This randomization procedure was repeated 1000 times to obtain a null

distribution of t statistics. To test whether the observed CTF selectivity was reliably above

chance, we calculated the probability of obtaining a t statistic from the surrogate null distribution

ALPHA OSCILLATIONS TRACK COVERT SPATIAL ATTENTION   16

greater than or equal to the observed t statistic (i.e., the probability of a Type 1 Error). Our

permutation test was therefore a one-tailed test. CTF selectivity was deemed reliably above

chance if the probability of a Type 1 Error was less than .01. This permutation testing procedure

was applied to each time-frequency point in the time-frequency analyses, and to each time point

in the alpha-band analyses.

Jackknife test for latency differences. In Experiment 2, we tested for differences in CTF

onset latency between easy search and hard search trials, and between trials with fast RTs and

trials with slow RTs. We used a jackknife-based procedure (Miller, Patterson, & Ulrich, 1998) to

test for latency difference in CTF onset. CTF onset latency was measured as the earliest time at

which CTF slope reached 50% of its maximum amplitude. The latency difference between

conditions, D, was measured as the difference in onset latency between conditions in the subject-

averaged CTF slope time-courses. The standard error of the latency difference, SE_D, was

estimated using a jackknife procedure (Miller et al., 1998), whereby SE_D was estimated from the

latency differences obtained for subsamples that included all but one subject. Specifically, the

latency differences, D_{-i}, for $i = 1, \ldots, N$ (where N is the sample size), were calculated where D_{-i}

was the latency difference for the sample with all subjects except for subject i. The jackknife

estimate of the standard error of the difference, SE_D, was calculated as:

$$SE_D = \sqrt{\frac{N-1}{N} \sum_{i=1}^{N} (D_{-i} - \bar{J})^2}$$

where $\bar{J}$ is the mean of the differences obtained for all subsamples (i.e., $\bar{J} = \sum D_{-i}/N$).

A jackknifed t statistic, t_j, was then calculated as:

$$t_j = \frac{D}{SE_D}$$

ALPHA OSCILLATIONS TRACK COVERT SPATIAL ATTENTION   17

which approximately follows a *t* distribution with *N* – 1 degrees of freedom under the null

hypothesis. Our jackknife tests for latency differences in CTFs onsets were one-tailed because

we had clear direction hypotheses: that CTF onset would be delayed for hard search compared

with easy search, and for trials with slow RTs compared with trials with fast RTs. The jackknife

approach to testing for latency differences between conditions circumvents the need to calculate

latency differences for individual subjects, which are often noisy due to the low signal-to-noise

ratio of EEG data (Miller et al. 1998).

Experiment 1

Subjects in Experiment 1 performed a spatial cueing task in which they identified a target

digit among distractor letters (Fig. 2a). A central cue indicated the likely location of the target

(valid on 87.5% of trials). We observed a robust spatial cueing effect in the accuracy of target

discrimination (Fig. 2b): target discrimination accuracy was higher on validly cued trials ($M =$

83.5%, $SD = 9.5\%$) than on invalidly cued trials ($M = 36.9\%$, $SD = 18.2\%$), $t(15) = 14.33$, $p <$

.001, Cohen's $d_z = 3.58$.

Having established that subjects attended the cued location, we tested whether the

topography of alpha-band activity tracked shifts of covert attention to the cued location

(collapsing across validly and invalidly cued trials). Using an IEM, we reconstructed spatial

CTFs from the scalp distribution of alpha power. A spatially selective CTF emerged several

hundred milliseconds after cue onset, sustaining until the search array was presented (Fig. 2c).

Figure 2d shows CTF selectivity across time (quantified as CTF slope, see General Method). A

permutation testing procedure revealed that CTF selectivity was reliably above chance starting

304 ms after cue onset. Therefore, covert attention must have been shifted to the cued location by

this time at the latest. The time-course of the attention-related CTF dovetails with past behavioral

ALPHA OSCILLATIONS TRACK COVERT SPATIAL ATTENTION   18

work, which has shown that endogenously cued shifts of attention typically take 200-400

milliseconds to execute (Cheal & Lyon, 1991; Eriksen & Collins, 1969; Liu, Stevens, &

Carrasco, 2007; Müller and Rabbit, 1989; Nakayama & Mackeben, 1989; for review, see Egeth

& Yantis, 1997).

Next, we examined whether alpha-band activity tracked the specific location that was

attended. The alpha CTFs that we have reported so far reflected channel response profiles that

were averaged across all possible cued locations. We observed reliable spatial selectivity in the

averaged CTF. Nevertheless, it is possible that the spatial selectivity of the averaged CTF

reflects selectivity for some locations but not others, leading to reliable spatial selectivity on

average (Foster et al., 2016). Thus, we inspected the alpha CTFs for each cued location

separately (Fig. 2e). For each location, the CTF peaked at the channel tuned for the cued location

(i.e., a channel offset of 0°) starting approximately 300 ms after cue onset, demonstrating that

time-resolved alpha CTFs tracked which of the eight locations was attended. Thus, alpha-band

activity tracks the locus of covert attention in a spatially precise fashion.

Alpha CTFs showed a graded response profile, with the strongest response in the channel

tuned for the cued location, and steadily decreasing responses across channel tuned for other

locations (Fig. 2f). However, our standard basis set specified a graded channel response profile.

Therefore, the graded profile of alpha CTFs might be imposed by the graded basis function

rather than reflecting truly graded spatially-selective activity. To test this possibility, we

reconstructed CTFs with the IEM again, with a basis set of Kronecker delta functions ('stick'

functions; Foster et al., 2016). These basis functions do not specify a graded channel response

profile. Thus, a graded CTF profile seen using this modified basis set necessarily reflects graded

activity in the data itself rather than a pattern imposed by the basis function. Alternatively, if

spatially-selective alpha activity does not follow a graded format, then we should recover a peak

in the channel tuned for the attended location, and uniform responses across the other channels.

Using this modified basis set, we found that alpha CTFs (averaged from 300-1250 ms) showed a

graded profile across channels (Fig. 2f), demonstrating that the graded profile of alpha CTFs

reflects the underlying spatial selectivity of covert spatial attention.

Having established that the topographic distribution of alpha power tracks the spatial

locus of covert attention, we tested whether such spatially selective activity is specific to the

alpha band (8-12 Hz). We used the IEM to search a range of frequencies (4-50 Hz, in increments

of 1 Hz) across time to identify the frequency bands in which the topographic distribution of

power carried information about the attended location (Fig. 2g). We found that spatially

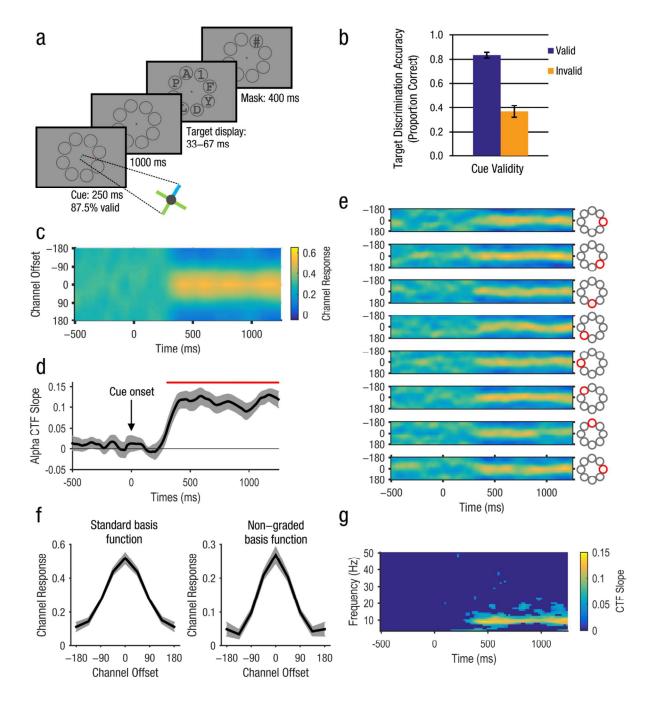selectivity oscillatory activity was largely restricted to the alpha band.

ALPHA OSCILLATIONS TRACK COVERT SPATIAL ATTENTION 20

Figure 2. Task and results from Experiment 1. Spatial cueing task used in Experiment 1 (a). A central cross cue (87.5% valid) directed subjects to attend one of eight placeholders. Subjects identified the target digit among distractor letters. Target discrimination accuracy was higher on validly cued trial than invalidly cued trials showing that subjects attended the cued location (b). The plot in (c) shows the average alpha CTF across time. The selectivity of the alpha CTF (measured as CTF slope) is show in (d). Reliable CTF selectivity (red marker in d) was evident, starting ~300 ms after cue onset (0 ms). Thus, alpha CTFs tracked orienting of covert spatial attention following the cue in this spatial cueing task. Panel (e) shows the CTFs for each of the eight cued locations separately. For each location, the peak response was seen in the channel tuned for that location (i.e., channel offset of 0°), demonstrating that the topography of alpha-

ALPHA OSCILLATIONS TRACK COVERT SPATIAL ATTENTION   21

band power tracked the specific location that was attended. Panel (f) shows the channel response profile recovered using the standard "graded" basis function (left) and an orthogonal, non-graded basis function (right). Both profiles are clearly graded, demonstrating that the underlying spatial tuning of alpha-band activity follows a graded pattern. The plot in (g) shows the slope of CTFs reconstructed from the topographic distribution of oscillatory power across a broad range of frequencies (4-50 Hz, in increments of 1 Hz). Points at which CTF slope were not reliable above zero as determined by a permutation test are set to zero (dark blue). Spatially specific activity was largely restricted to the alpha-band. All shaded error bars reflect bootstrapped standard error of the mean.

Experiment 2

In Experiment 1, we showed that spatially selective CTFs can be reconstructed from the topographic distribution of alpha power following a central, attention-directing cue. This spatially selective activity emerged several hundred milliseconds after cue onset, dovetailing with behavioral estimates of the time-course of endogenous shifts of spatial attention (e.g., Müller & Rabbit, 1989). While this finding suggests that alpha CTFs track spatial attention in a temporally resolved fashion, a direct test requires a manipulation of covert orienting speed. In Experiment 2 we manipulated the speed of target selection during visual search. Subjects performed a visual search task in which they searched for a target (a horizontal or vertical bar) among distractors (Fig. 3a). We varied the difficulty of search by manipulating both distractor variability and target-distractor similarity (Duncan & Humphreys, 1989), and measured reaction time to obtain a trial-by-trial estimate of the time taken to attend the target. This approach allowed us to test whether the time-course of alpha-based CTFs tracks differences in the latency of target selection across different levels of search difficulty, and as a function of within-subject differences in orienting latency across trials.

Figure 3b shows the aggregate RT distributions for easy and hard search. Our manipulation of search difficulty was effective: median RTs were slower for hard search ($M =$ 829, $SD = 153$) than for easy search ($M = 593$, $SD = 71$), $t(22) = 12.31$, $p < .001$, Cohen's $d_z =$

ALPHA OSCILLATIONS TRACK COVERT SPATIAL ATTENTION　　　　　　　22

2.57, and accuracy was lower for hard search (M = 91.7%, SD = 4.4%) than for easy search (M = 97.0% , SD = 2.4%), $t(22) = 6.09$, $p < .001$, Cohen's $d_z = 1.27$. We first tested whether alpha CTFs tracked orienting to the target location during the visual search task. As in Experiment 1, we quantified the spatial selectivity of alpha CTFs and CTF slope (see General Methods). A spatially selective alpha CTF emerged soon after onset of the search array (Fig 3c). A permutation testing procedure revealed that CTF selectivity was reliably above chance starting 196 ms after cue onset. Thus, alpha CTFs tracked covert orienting to the target's location during visual search. To test whether alpha CTFs track the *latency* of covert orienting to the search target, we compared the onset latency of target-related CTFs between the easy and hard search conditions. To measure the difference in onset latency of target-related CTF between the search conditions (easy vs. hard), we used a jackknife-based procedure with a 50% maximum amplitude criterion (Miller et al., 1998; see General Method). The filled circles in Figure 3d mark the CTF onset estimates during easy and hard search. The difference in CTF onset of 440 ms was reliable, $t(22) = 2.48$, $p = .011$, Cohen's $d_z = 0.52$ (one-tailed test). Thus, the onset latency of the target-related CTF was delayed in the hard search compared with easy search, demonstrating that alpha-based CTFs reveal the difference in the latency of orienting attention to the target between the search conditions.

While RTs were generally slower for hard search than for easy search, there was also considerable overlap in RTs between the easy and hard condition (Fig. 3b). This overlap was expected because target selection should sometimes occur very quickly during hard search, when the target happens to be one of the initial items to be selected. Given the overlap in RTs between conditions, we examined the onset latency of target-related CTFs split by RT, comparing the 50% of trials with the fastest RTs (*fast trials*) with the 50% of trials with the slowest RTs (*slow*

ALPHA OSCILLATIONS TRACK COVERT SPATIAL ATTENTION   23

trials), regardless of search condition (Fig. 3e). If alpha CTFs reveal the latency of target

selection, CTF latency should covary with trial-by-trial reaction times. Indeed, we found the

target-related CTF onset 372 ms later for slow trials than for fast trials, $t(22) = 7.22$, $p < .001$,

Cohen's $d_z = 1.51$ (one-tailed test), providing further evidence that the onset of target-related

CTFs track the latency of covert orienting to the target item during visual search.
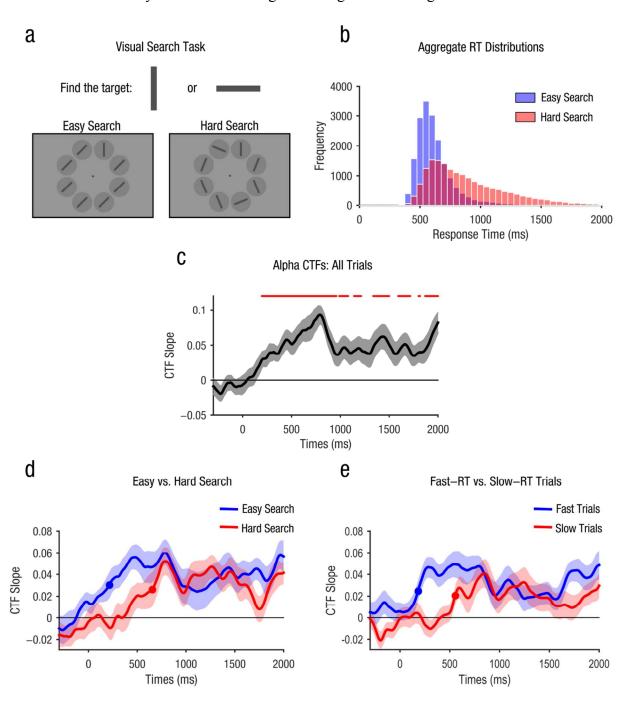
ALPHA OSCILLATIONS TRACK COVERT SPATIAL ATTENTION   24

Figure 3. Task and results from Experiment 2. Subjects in Experiment 2 searched for a target (a vertical or horizontal bar) among distractors and reported the target's orientation (a). Search difficulty (easy vs. hard) was varied by manipulating distractor variability and target-distractor similarity. The histogram in (b) shows aggregate response time (RT) histograms for easy and hard search. Median RTs were faster for easy search than for hard search. Nevertheless, there was considerable overlap in RTs between the search conditions. The plot in (c) show selectivity of the target-related alpha CTF (measured as CTF slope) across time, collapses across the search conditions (easy and hard). Reliable CTF selectivity (red marker) was evident, starting ~200 ms after onset of the search array (0 ms). The plots in (d) and (e) shows target-related CTF slope across time for easy and hard search, and for fast vs. slow RT trials (regardless of search condition). Filled circles mark the point at which the target-related CTF reached the onset criterion (50% of maximum amplitude). Onset latency was delayed during Hard Search compared with Easy Search (d), and for slow-RT trials compared with fast-RT trials (e), demonstrating that the onset of target-related CTFs tracked the latency of orienting to the search target. Shaded error bars in plots (c-e) reflect bootstrapped standard error of the mean.

Discussion

The central role of covert spatial attention in visual cognition has motivated a sustained effort to elucidate the neural mechanisms that underpin this process. One productive avenue has been to examine the links between oscillatory alpha-band activity and spatial attention. A growing body of evidence has shown that the topographic distribution of alpha power tracks the locus of spatial attention (e.g., Kelly et al., 2006; Rihs et al., 2007; Thut et al., 2006; Worden et al., 2000), suggesting that alpha oscillations play a role in biasing visual processing towards attended locations (Foxe & Snyder, 2011; Jensen & Mazaheri, 2010). This view makes another clear prediction that had not been subjected to a rigorous test: that the topographic distribution of alpha power should track the temporal dynamics of covert spatial attention.

Our findings provide a compelling confirmation of this prediction. In Experiment 1, we showed that variations in scalp distribution of alpha power enable the reconstruction of spatially specific response profiles (called channel tuning functions of CTFs) that track the endogenous orienting of spatial attention following a central cue. These alpha CTFs precisely discriminated the attended position starting approximately 300 ms after the onset of the central cue, consistent

with past estimates of the time taken to endogenously shift attention (e.g., Müller and Rabbit, 1989; Nakayama & Mackeben, 1989; for review, see Egeth & Yantis, 1997). Critically, Experiment 2 extended this finding by showing that dynamic changes in alpha topography tracked the latency of covert orienting during visual search. The onset of alpha CTFs was delayed during difficult search compared with easy search, and for trials with slow responses compared with fast responses. Together these findings demonstrate that moment-by-moment changes in the topography of alpha-band activity track the temporal dynamics of covert spatial attention, closing a significant gap in the evidence linking alpha activity with covert spatial orienting.

Experiment 2 also provides important evidence that spatially specific alpha-band activity plays a role in covert spatial attention in a range of paradigms. It has long been thought that covert spatial orienting plays a central role in visual search (e.g., Kim & Cave, 1995; Luck, Fan, & Hillyard, 1993). However, evidence linking alpha-band activity to covert orienting during visual search has been lacking because studies that have linked alpha-band activity with spatial attention have relied almost exclusively on spatial cueing tasks (e.g., Thut et al, 2006; Worden et al., 2000). Our finding that alpha CTFs tracked the latency of orienting to a target during visual search provide clear evidence for the role of alpha-band activity in visual search. Thus, spatially specific alpha-band activity plays a general role in covert orienting in a range of paradigms.

Our findings also have important methodological implications for a field that has had a longstanding interest in the spatial and temporal dynamics of covert orienting (Egeth & Yantis, 1997). Early work relied on overt behavioral responses to probe these dynamics (e.g., Downing, 1998; Müller & Rabbit, 1989). More recently, however, neural signals that track the allocation of attention have played a central role in this endeavor, in part because they circumvent the need for

ALPHA OSCILLATIONS TRACK COVERT SPATIAL ATTENTION   26

overt behavioral responses. Functional magnetic resonance imaging (fMRI) precisely tracks the

spatial locus of covert attention (e.g., Brefczynski & DeYoe, 1999; Tootell et al., 1998) but

provides little information about the time-course of attention because of the slow hemodynamic

response. Thus, researchers have relied on electrophysiological signals to examine the temporal

dynamics of attention (e.g., Garcia, Srinivasan, & Serences, 2013; Müller, Teder-Sälejärvi,

Hillyard, 1998).

One productive approach has been to measure the *consequences* of spatial attention by

examining stimulus-evoked potentials, rather than measuring endogenous, attention-related

activity directly. Sensory components that are amplified by spatial attention (e.g., the P1

component; Hillyard, Luck, & Vogel, 1998), have allowed researchers to probe the spatial

allocation of attention. For example, Hopfinger and Mangun (1998) showed that the P1 response

evoked by a probe stimulus was amplified following an exogenous spatial cue, showing that

exogenous orienting shapes early stages of visual processing. However, while this approach has

provided important insights into how and when attention modulates evoked visual responses, it

does not reveal the time-course of covert orienting prior to the evoking stimulus. To overcome

this limitation, some studies have focused on the rhythmic brain activity that is evoked by a

flickering stimulus (called a steady state visual evoked potential or SSVEP). The SSVEP is

amplified by spatial attention (Morgan, Hansen, & Hillyard, 1996). Thus, by examining the time-

course of amplitude modulations, it has been possible to measure the latency of orienting

towards a flickering target (e.g., Müller et al. 1998). Nevertheless, stimulus-evoked approaches

are not without limitations. Most notably, because these approaches rely on stimulus-evoked

activity they cannot be used to track attention to empty locations, restricting the kinds of

questions that can be addressed with these methods. Thus, there is much to be gained from a

temporally-resolved signal that tracks spatial attention in the absence stimulus-evoked activity.

Our findings suggest that spatially specific alpha-band activity provides such an

opportunity. Alpha CTFs tracked the locus of covert spatial attention in balanced visual displays

and in the absence of transient evoked activity, suggesting that spatially specific alpha-band

activity reflects endogenous shifts of spatial attention rather than stimulus-evoked activity. Thus,

given its spatial and temporal precision, this method provides a promising approach for obtaining

a moment-by-moment index of the locus of covert attention across a broad range of paradigms.

Conclusions

Here, we showed that the topographic distribution of alpha-band activity tracks the

spatial locus of covert attention following attention-directing cues, and during visual search,

demonstrating that alpha-band activity plays a central role in covert orienting in a range of

paradigms. Critically, the time-course of spatially specific alpha activity tracked trial-by-trial

variations in the speed of covert orienting during visual search. Our results provide critical new

evidence for the link between alpha-band activity and covert spatial attention.

ALPHA OSCILLATIONS TRACK COVERT SPATIAL ATTENTION   28

References

Bahramisharif, A., Van Gerven, M., Heskes, T., & Jensen, O. (2010). Covert attention allows for continuous control of brain–computer interfaces. *European Journal of Neuroscience, 31*(8), 1501-1508. doi:10.1111/j.1460-9568.2010.07174.x

Brainard, D. H. (1997). The psychophysics toolbox. *Spatial Vision, 10*(4), 433-436. doi:http://dx.doi.org/10.1163/156856897X00357

Brefszynski, J.A., & DeYoe, E.A., (1999). A physiological correlate of the 'spotlight' of visual attention. *Nature Neuroscience, 2*(4), 370-374. doi:10.1038/7280

Brouwer, G. J., & Heeger, D. J. (2009). Decoding and reconstructing color from responses in human visual cortex. *The Journal of Neuroscience, 29*(44), 13992-14003. doi:10.1523/JNEUROSCI.3577-09.2009

Carrasco, M. (2011). Visual attention: The past 25 years. *Vision Research, 51*(13), 1484-1525. doi: 10.1016/j.visres.2011.04.012

Carrasco, M., & McElree, B. (2000). Covert attention accelerates the rate of visual information processing. *Proceedings of the National Academy of Sciences, 98*(9), 5363-5367. doi:10.1073/pnas.081074098

Cheal, M., & Lyon, D. R. (1991). Central and peripheral precuing of forced-choice discrimination. *Quarterly Journal of Experimental Psychology, 43A*(4), 859-880. doi:10.1080/14640749108400960

Delorme, A., & Makeig, S. (2004). EEGLAB: an open source toolbox for analysis of single-trial EEG dynamics including independent component analysis. *Journal of Neuroscience Methods, 134*(1), 9-21. doi:10.1016/j.jneumeth.2003.10.009

ALPHA OSCILLATIONS TRACK COVERT SPATIAL ATTENTION   29

Downing, C. J. (1988). Expectancy and visual-spatial attention: effects on perceptual quality.

   Journal of Experimental Psychology: Human Perception and Performance, 14(2), 188-

   202. doi:10.1037/0096-1523.14.2.188

Duncan, J., & Humphreys, G. W. (1989). Visual search and stimulus similarity. *Psychological

   Review, 96*(3), 433-458. doi:10.1037/0033-295x.96.3.433

Egeth, H. E., & Yantis, S. (1997). Visual attention: control, representation, and time course.

   Annual Review of Psychology, 48, 269-297. doi:10.1146/annurev.psych.48.1.269

Eriksen, C. W., & Collins, J. F. (1969). Temporal course of selective attention. *Journal of

   Experimental Psychology, 80*(2), 254-261. doi:10.1037/h0027268

Eriksen, C. W., & Hoffman, J. E. (1974). Selective attention: Noise suppression or signal

   enhancement? *Bulletin of the Psychonomic Society*, *4*(6), 587-589.

   doi:10.3758/bf03334301

Foster, J. J., Sutterer, D. W., Serences, J. T., Vogel, E. K., & Awh, E. (2016). The topography of

   alpha-band activity tracks the content of spatial working memory. *Journal of

   Neurophysiology, 115*(1), 168-177. doi:10.1152/jn.00860.2015

Foxe, J. J., & Snyder, A. C. (2011). The role of alpha-band brain oscillations as a sensory

   suppression mechanism during selective attention. *Frontiers in Psychology*, *2*, 154.

   doi:10.3389/fpsyg.2011.00154

Garcia, J.O., Srinivasan, R., & Serences, J.T. (2013). Near-real-time feature-selective

   modulations in human cortex. *Current Biology, 23*(6), 512-522.

   doi:10.1016/j.cub.2013.02.013

Hillyard, S.A., Vogel, E.K., & Luck, S.J. (1998). Sensory gain control (amplification) as a

   mechanism of selective attention: electrophysiological and neuroimaging evidence.

ALPHA OSCILLATIONS TRACK COVERT SPATIAL ATTENTION
30

Philosophical Transactions of the Royal Society B: Biological Sciences, 353(1373), 1257-1270. doi:10.1098/rstb.1998.0281

Hopfinger, J.B., & Mangun, G.R. (1998). Reflexive attention modulates processing of visual stimuli in human extrastriate cortex. *Psychological Science, 9*(6), 441-447. doi:10.1111/1467-9280.00083

Jensen, O., & Mazaheri, A. (2010). Shaping functional architecture by oscillatory alpha activity: gating by inhibition. *Frontiers in Human Neuroscience, 4*, 186. doi:10.3389/fnhum.2010.00186

Kelly, S. P., Lalor, E. C., Reilly, R. B., & Foxe, J. J. (2006). Increases in alpha oscillatory power reflect an active retinotopic mechanism for distracter suppression during sustained visuospatial attention. *Journal of Neurophysiology, 95*(6), 3844-3851. doi:10.1152/jn.01234.2005

Kim, M. S., & Cave, K. R. (1995). Spatial attention in visual search for features and feature conjunctions. *Psychological Science, 6*(6), 376-380. doi:10.1111/j.1467-9280.1995.tb00529.x

Lins, O. G., Picton, T. W., Berg, P., & Scherg, M. (1993). Ocular artifacts in EEG and event-related potentials. I: Scalp topography. *Brain Topography, 6*(1), 51-63. doi:10.1007/BF01234127

Liu, T., Stevens, S. T., & Carrasco, M. (2007). Comparing the time course and efficacy of spatial and feature-based attention. *Vision Research, 47*(1), 108-113. doi:10.1016/j.visres.2006.09.017

ALPHA OSCILLATIONS TRACK COVERT SPATIAL ATTENTION   31

Luck, S. J., Fan, S., & Hillyard, S. A. (1993). Attention-related modulation of sensory-evoked

brain activity in a visual search task. *Journal of Cognitive Neuroscience,5*(2), 188-195.

doi:10.1162/jocn.1993.5.2.188

Morgan, S. T., Hansen, J. C., & Hillyard, S. A. (1996). Selective attention to stimulus location

modulates the steady-state visual evoked potential. *Proceedings of the National Academy

of Science, 93*(10), 4770-4774. Retrieved from: http://www.pnas.org

Miller, J., Patterson, T., & Ulrich, R. (1998). Jackknife-based method for measuring LRP onset

latency differences. *Psychophysiology, 35*(1), 99-115. doi: 10.1111/1469-8986.3510099

Müller, H. J., & Rabbitt, P. M. (1989). Reflexive and voluntary orienting of visual attention: time

course of activation and resistance to interruption. *Journal of Experimental Psychology:

Human Perception and Performance, 15*(2), 315-330. doi:10.1037/0096-1523.15.2.315

Müller, M. M., Teder-Sälejärvi, W., & Hillyard, S. A. (1998). The time course of cortical

facilitation during cued shifts of spatial attention. *Nature Neuroscience, 1*(7), 631-634.

doi:10.1038/2865

Nakayama, K., & Mackeben, M. (1989). Sustained and transient components of focal visual

attention. *Vision Research, 29*(11), 1631-1647. doi:10.1016/0042-6989(89)90144-2

Pelli, D. G. (1997). The VideoToolbox software for visual psychophysics: Transforming

numbers into movies. *Spatial Vision, 10*(4), 437-332. doi:10.1163/156856897X00366

Posner, M. I. (1980). Orienting of attention. *Quarterly Journal of Experimental Psychology,

32*(1), 3-25. doi:10.1080/00335558008248231

Rihs, T. A., Michel, C. M., & Thut, G. (2007). Mechanisms of selective inhibition in visual

spatial attention are indexed by α-band EEG synchronization. *European Journal of

Neuroscience, 25*(2), 603-610. doi: 10.1111/j.1460-9568.2007.05278.x

ALPHA OSCILLATIONS TRACK COVERT SPATIAL ATTENTION   32

Samaha, J., Sprague, T. C., & Postle, B. R. (2016). Decoding and reconstructing the focus of

spatial attention from the topography of alpha-band oscillations. *Journal of Cognitive*

Neuroscience, 28(8), 1090-1097. doi:10.1162/jocn_a_00955

Sauseng, P., Klimesch, W., Stadler, W., Schabus, M., Doppelmayr, M., Hanslmayr, S., …

Birbaumer, N. (2005). A shift of visual spatial attention is selectively associated with

human EEG alpha activity. *European Journal of Neuroscience*, *22*(11), 2917-2926.

doi:10.1111/j.1460-9568.2005.04482.x

Sprague, T. C., Saproo, S., & Serences, J. T. (2015). Visual attention mitigates information loss

in small- and large-scale neural codes. *Trends in Cognitive Sciences, 19*(4), 215-226.

doi:10.1016/j.tics.2015.02.005

Sprague, T. C., & Serences, J. T. (2013). Attention modulates spatial priority maps in the human

occipital, parietal and frontal cortices. *Nature neuroscience, 16*(12), 1879-1887.

doi:10.1038/nn.3574

Thut, G., Nietzel, A., Brandt, S. A., & Pascual-Leone, A. (2006). α-band

electroencephalographic activity over occipital cortex indexes visuospatial attention bias

and predicts visual target detection. *Journal of Neuroscience, 26*(37), 9494-9502.

doi:10.1523/JNEUROSCI.0875-06.2006

Tootell, R. B., Hadjikhani, N., Hall, E. K., Marrett, S., Vanduffel, W., Vaughan, J. T., & Dale, A.

M. (1998). The retinotopy of visual spatial attention. *Neuron, 21*(6), 1409-1422.

doi:10.1016/s0896-6273(00)80659-5

Worden, M. S., Foxe, J. J., Wang, N., & Simpson, G. V. (2000). Anticipatory biasing of

visuospatial attention indexed by retinotopically specific α-band electroencephalography

ALPHA OSCILLATIONS TRACK COVERT SPATIAL ATTENTION   33

increases over occipital cortex. *Journal of Neuroscience, 20,* RC63. Retrieved from:

http://www.jneurosci.org/

ALPHA OSCILLATIONS TRACK COVERT SPATIAL ATTENTION   34

Footnotes

[1] Three additional volunteers completed the practice session for Experiment 2 (see Procedures) but did not return for the EEG session.

[2] For experiment 1 our target sample size was 16 subjects, following our previous work using the method we used here to tracks locations held in spatial working memory (Foster et al., 2016).

[3] For experiment 2, our target sample was a minimum of 20 subjects. Our target sample size was larger for Experiment 2 than for Experiment 1 because we had not run comparable tests for latency differences in previous work. Our lab was soon to relocate at the time of data collection. Thus, we continued data collection beyond our minimum sample until we no longer had access to the apparatus.

1
2
3
4
5
6
7
8
9
10
11
12
13
14
15
16
17
18
19
20
21
22
23
24
25
26
27
28
29
30
31
32
33
34
35
36
37
38
39
40
41
42
43
44
45
46
47
48
49
50
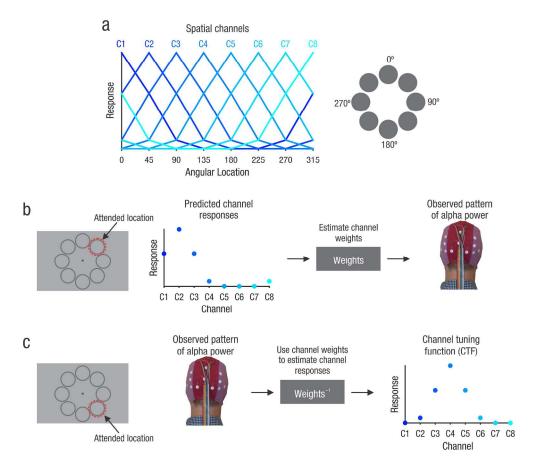51
52
53
54
55
56
57
58
59
60

Figure 1. Inverted encoding method for reconstructing spatial channel tuning functions (CTFs) from the pattern of alpha-band (8-12 Hz) power across the scalp. We modeled alpha power measured at each electrode as the weighted sum of eight spatially tuned channels (a). Each curve shows the predicted response of one of the channels across eight possible attended angular locations. In a training phase (b), we estimated a set of channel weights that characterize the relative contributions of each of the spatial channels to the response measured at each of the scalp electrodes. In a test phase (c), using an independent set of data, we used the channel weights to estimate the channel responses from the observed pattern of alpha power on the scalp. The resulting channel tuning function (CTF) reflects the spatial selectivity of population-level alpha power, as measured with EEG.
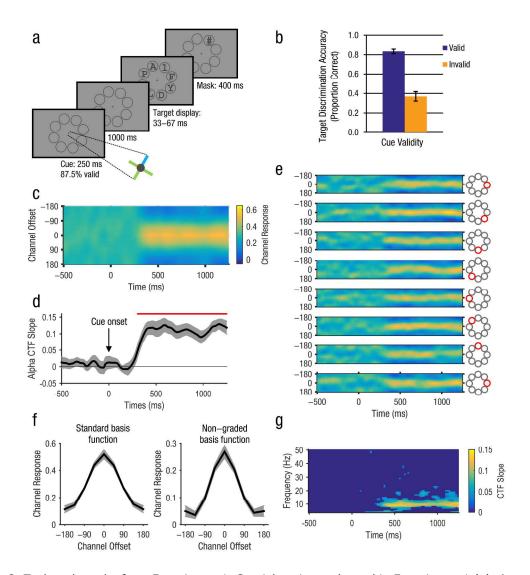
151x132mm (600 x 600 DPI)

Figure 2. Task and results from Experiment 1. Spatial cueing task used in Experiment 1 (a). A central cross cue (87.5% valid) directed subjects to attend one of eight placeholders. Subjects identified the target digit among distractor letters. Target discrimination accuracy was higher on validly cued trial than invalidly cued trials showing that subjects attended the cued location (b). The plot in (c) shows the average alpha CTF across time. The selectivity of the alpha CTF (measured as CTF slope) is show in (d). Reliable CTF selectivity (red marker in d) was evident, starting ~300 ms after cue onset (0 ms). Thus, alpha CTFs tracked orienting of covert spatial attention following the cue in this spatial cueing task. Panel (e) shows the CTFs for each of the eight cued locations separately. For each location, the peak response was seen in the channel tuned for that location (i.e., channel offset of 0°), demonstrating that the topography of alpha-band power tracked the specific location that was attended. Panel (f) shows the channel response profile recovered using the standard "graded" basis function (left) and an orthogonal, non-graded basis function (right). Both profiles are clearly graded, demonstrating that the underlying spatial tuning of alpha-band activity follows a graded pattern. The plot in (g) shows the slope of CTFs reconstructed from the topographic distribution of oscillatory power across a broad range of frequencies (4-50 Hz, in increments of 1 Hz). Points at which CTF slope were not reliable above zero as determined by a permutation test are set to zero (dark blue). Spatially specific activity was largely restricted to the alpha-band. All shaded error bars reflect bootstrapped standard error of the mean.

190x199mm (600 x 600 DPI)

1
2
3
4
5
6
7
8
9
10
11
12
13
14
15
16
17
18
19
20
21
22
23
24
25
26
27
28
29
30
31
32
33
34
35
36
37
38
39
40
41
42
43
44
45
46
47
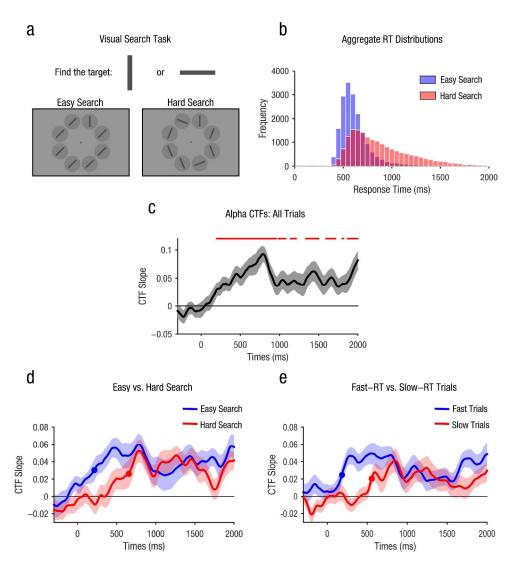48
49
50
51
52
53
54
55
56
57
58
59
60

Figure 3. Task and results from Experiment 2. Subjects in Experiment 2 searched for a target (a vertical or horizontal bar) among distractors and reported the target's orientation (a). Search difficulty (easy vs. hard) was varied by manipulating distractor variability and target-distractor similarity. The histogram in (b) shows aggregate response time (RT) histograms for easy and hard search. Median RTs were faster for easy search than for hard search. Nevertheless, there was considerable overlap in RTs between the search conditions. The plot in (c) show selectivity of the target-related alpha CTF (measured as CTF slope) across time, collapses across the search conditions (easy and hard). Reliable CTF selectivity (red marker) was evident, starting ~200 ms after onset of the search array (0 ms). The plots in (d) and (e) shows target-related CTF slope across time for easy and hard search, and for fast vs. slow RT trials (regardless of search condition). Filled circles mark the point at which the target-related CTF reached the onset criterion (50% of maximum amplitude). Onset latency was delayed during Hard Search compared with Easy Search (d), and for slow-RT trials compared with fast-RT trials (e), demonstrating that the onset of target-related CTFs tracked the latency of orienting to the search target. Shaded error bars in plots (c-e) reflect bootstrapped standard error of the mean.

184x197mm (600 x 600 DPI)

1
2
3
4
5
6
7
8
9
10
11
12
13
14
15
16
17
18
19
20
21
22
23
24
25
26
27
28
29
30
31
32
33
34
35
36
37
38
39
40
41
42
43
44
45
46
47
48
49
50
51
52
53
54
55
56
57
58
59
60